

810 A APPENDIX

811 A.1 IMPLEMENTATION DETAILS

812 The 2D occupancy map’s resolution is 5cm. For each single frontier pixel on the 2D map, we add 200
 813 3D Gaussians, which are uniformly distributed in the 3D cube above it. Other parameters like color,
 814 opacity, and scale are generated uniformly between 0 and 1. When there are frontiers on 2D map, we
 815 choose the next frontier to be explored by the area of each frontier divided by the distance. When
 816 no frontier exists, we select the top 20% of Gaussians with the highest score. These Gaussians are
 817 grouped using DBSCAN [9]. The largest cluster is selected for candidate pose generation. Candidates
 818 are uniformly sampled in the range between 0.3m to 1m, facing towards the selected position. Only
 819 the poses in free space are kept for path-level selection. The importance factor η in Eq. [7] is set
 820 to 5 across all experiments. The source code for this project will be made public no later than the
 821 publication of this paper.

822 We compute the Expected Information Gain (EIG) for each global candidate and use A* to plan a
 823 path for each of them. In order to prevent a twisted path, we consider locations 0.15m (3 pixels) away
 824 from the current robot position as neighbors and set the robot width to 3 pixels for collision check.
 825 However, the path planned by A* might have redundant waypoints, causing unnecessary turns for
 826 the robot. Therefore, we smooth the path by finding shortcuts. Specifically, for each waypoint w_i , if
 827 the path between waypoint w_{i+2} and w_i is collision-free, then we remove the intermediate waypoint
 828 w_{i+1} from the path. Finally, we use a greedy follower for motion planning. If the angle between the
 829 heading direction of the robot and the relative next waypoint is larger than 5° , then we turn left or
 830 right to decrease the angle. Otherwise, we choose the forward action to approach the next waypoint.
 831 In such a way, we get a sequence of actions $\{a_i\}_{i=1}^T$ for each path.

832 Given a sequence of actions $\{a_i\}_{i=1}^T$ for each path, we use forward dynamics to compute the future
 833 camera poses $\{c_i\}_{i=1}^T$. Initially, we use an intermediate variable $\mathbf{H}''_{\text{obs}} \triangleq \mathbf{H}''[\mathbf{w}^*]$ to help compute
 834 expected information gain along the path. For each camera pose x_i , we compute its pose Hessian
 835 $\mathbf{H}''_{\text{pose}}$ and the current model Hessian matrix $\mathbf{H}''_{\text{cur}} \triangleq \mathbf{H}''[\mathbf{y}|x_i, \mathbf{w}^*]$. $\mathbf{H}''_{\text{cur}}$ is then accumulated, and
 836 we update $\mathbf{H}''_{\text{obs}}$ to evaluate the remaining poses on the path. We select the path that minimizes the
 837 objective given by Eq. [7] for execution.

840 A.2 RESULTS FOR EACH SCENE IN GIBSON AND HM3D DATASET

841 Following previous literature [6], we use the following scenes for Gibson Dataset: Greigsville,
 842 Denmark, Cantwell, Eudora, Pablo, Ribera, Swormville, Eastville,
 843 Elmira. For HM3D we use the following scenes: DBjEChFg4oq, mscxX4KEBcB,
 844 QKGMrurUVbk, oPj9qMxrDEa, CETmJJqkhcK. The detailed results for each scene on each
 845 evaluation metric are presented as bar plots in Fig. [6] for Gibson and Fig. [7] for HM3D. We also
 846 present qualitative comparisons on testing views from the Gibson dataset in Fig. [8].

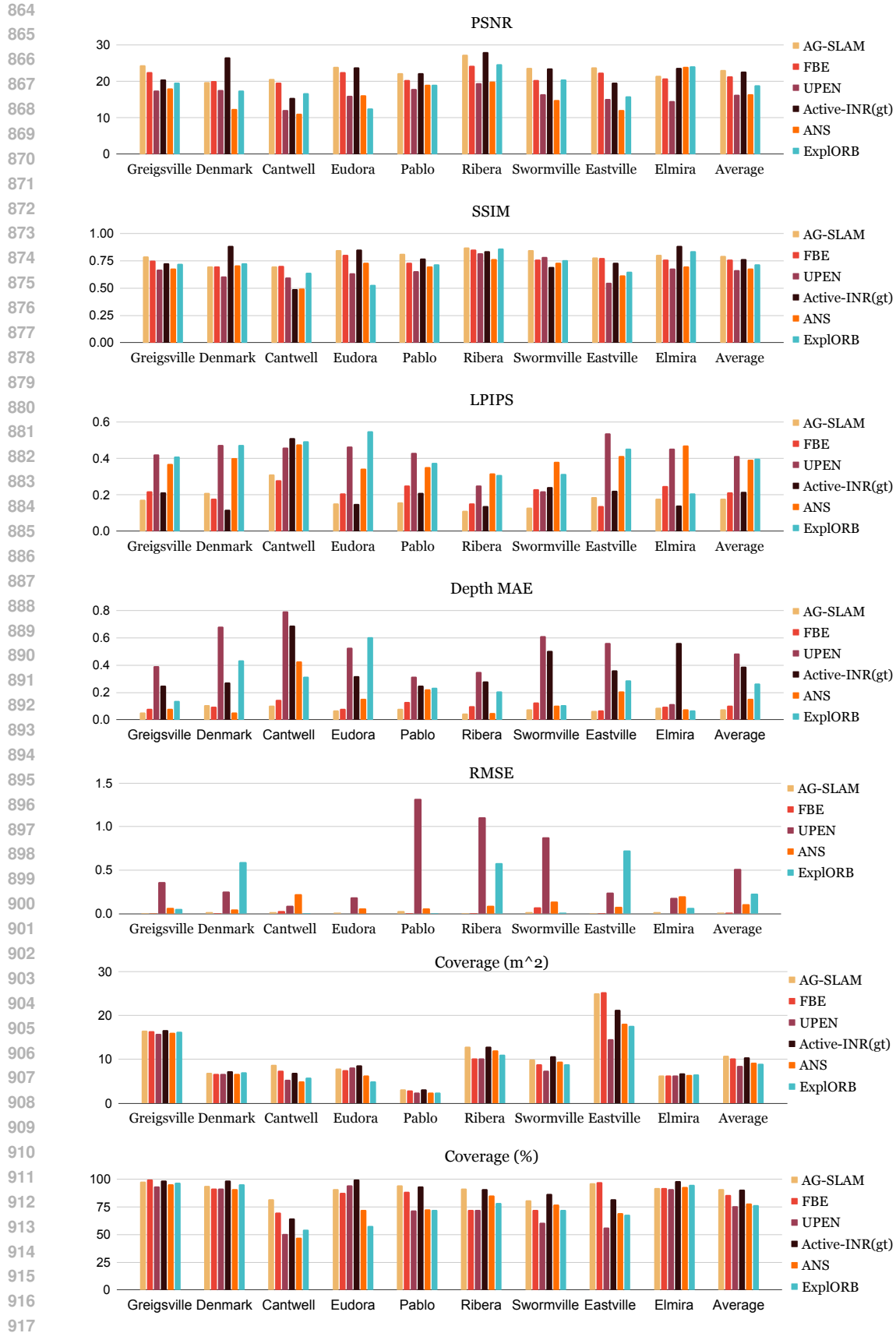


Figure 6: Per-scene results on Gibson Dataset

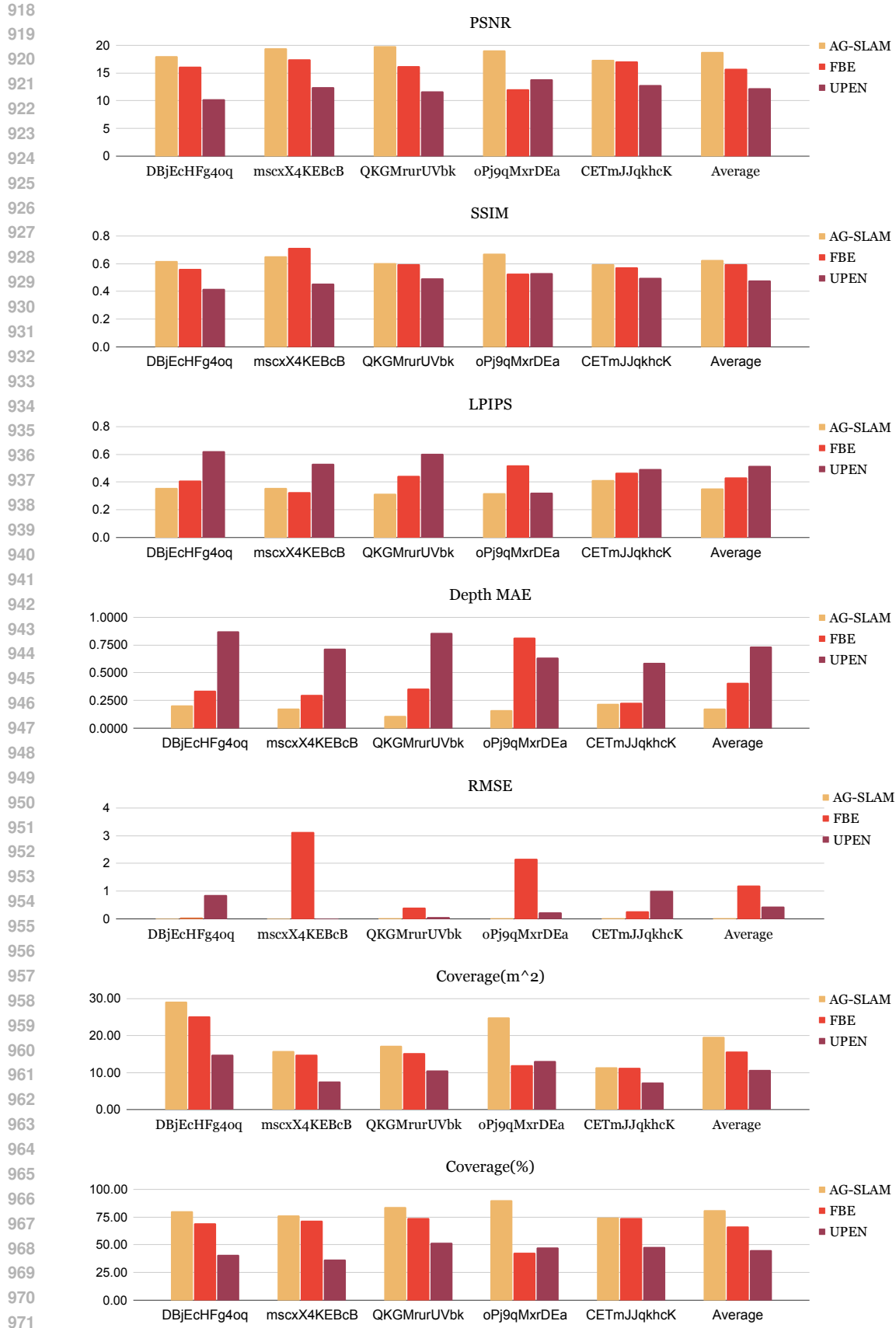


Figure 7: Per-scene results on HM3D Dataset

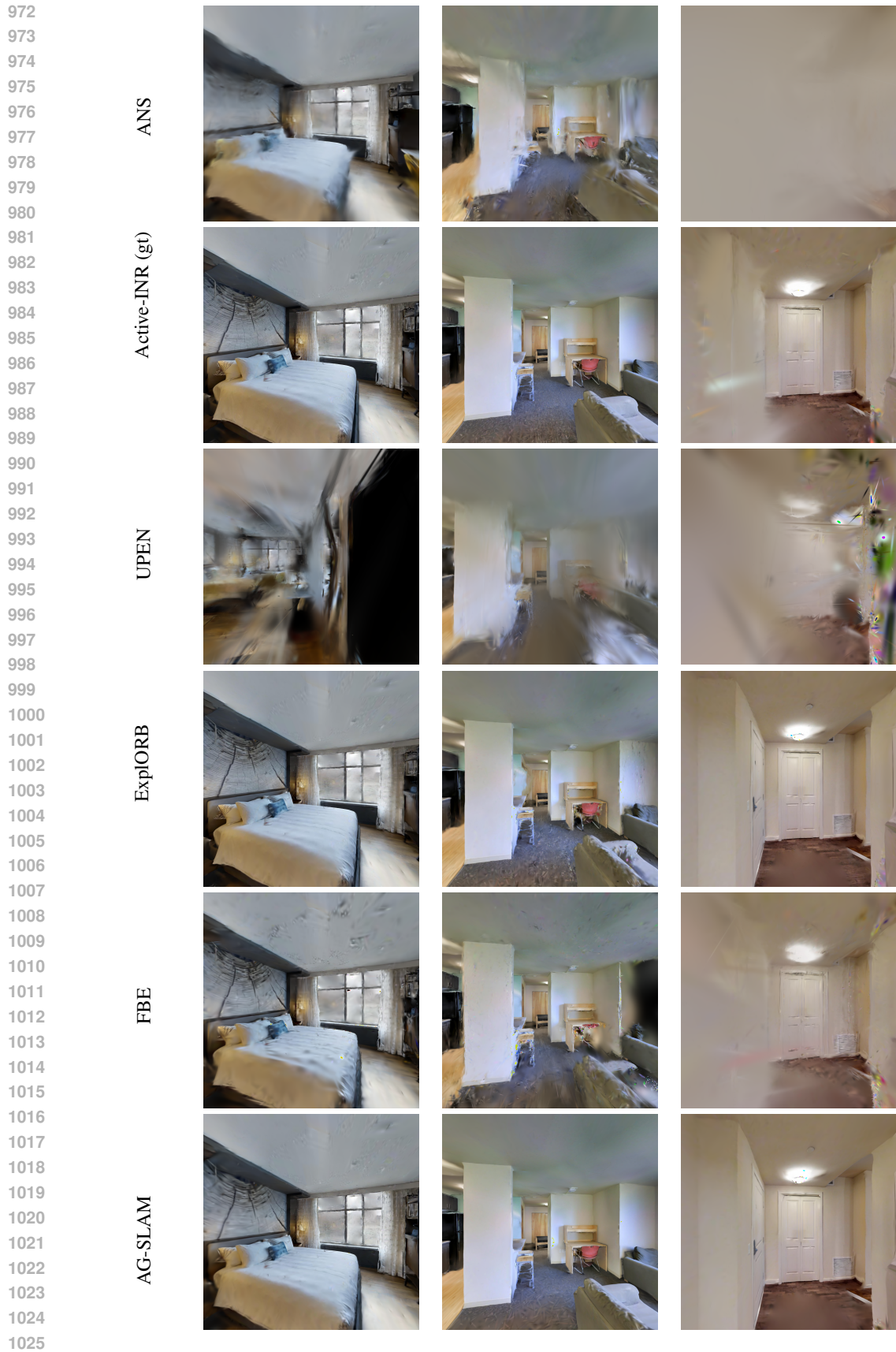


Figure 8: Test Rendering Qualitative Visualization on Gibson Dataset All the renderings are from the test view of the Gibson dataset.